

UDC 577.21

## The Formation of a Quaternary Structure by Recombinant Analogs of Spider Silk Proteins

O. S. Sokolova<sup>a</sup>, V. G. Bogush<sup>b</sup>, L. I. Davydova<sup>b</sup>, S. V. Polevova<sup>a</sup>, S. A. Antonov<sup>a</sup>, T. V. Neretina<sup>c</sup>,  
D. V. Klinov<sup>c</sup>, V. G. Debabov<sup>b</sup>, and M. P. Kirpichnikov<sup>a</sup>

<sup>a</sup> *Biological Department, Moscow State University, Moscow, 119991 Russia*  
*e-mail: sokolova@moldyn.org*

<sup>b</sup> *State Research Center GosNIIGenetika, Moscow, 113545 Russia*

<sup>c</sup> *Shemyakin and Ovchinnikov Institute of Bioorganic Chemistry, Russian Academy of Sciences, 117997 Russia*

Received February 20, 2009

Accepted for publication April 16, 2009

**Abstract**—The morphology of the fibers formed by recombinant analogs of dragline spider silk proteins, spidroins 1 and 2, was studied. It has been shown that the extension of the initial fiber, the so-called as-spun fiber, leads to remodeling of the spongy matrix with the formation of microfibrils, which is accompanied by a decrease in the fiber diameter. The breaking strength of the fiber depends not only on the primary structure of the constituent protein, but also on the way it was formed. Simulation of the assembly of microfibrils and the fibers formed of them can clarify the natural spider web spinning and enhance the development of technology for producing biomaterials with unique properties.

**DOI:** 10.1134/S0026893310010188

**Key words:** recombinant proteins, spidroins, scanning electron microscopy, transmission electron microscopy, microfibrils

The unique properties of spider web have attracted the attention of research for a long time. The dragline spider silk fibers combine a high mechanical resistance and resilience; their breaking strength is higher than that of steel, and the tensile energy is higher than that of Kevlar and nylon [1, 2]. The spider silk fibers are resistant to various chemical agents and compatible with living tissues.

The properties of spider and silkworm silk fibers have been intensively studied during the last 5–7 years due to their potential for medicine [3–5].

The dragline spider silk fiber consists of two proteins, spidroins 1 and 2, which have a high molecular weight and contain a large number of direct repeats [1, 2]. These repeats differ in the number of deletions and insertions yet have the same structural pattern: each contains a poly(Ala) element (4–10 amino acid residues), which render the protein hydrophobic, and a more hydrophilic Gly-rich sequence. Such alternation of hydrophilic and hydrophobic segments, as has been found, is of the utmost importance for solubility of these proteins. Due to the “retained” water, this alternation prevents a premature crystallization and is involved in the regulation of the lateral aggregation of molecules, leading to assembly of nanofibers [6, 7]. An ever increasing volume of data suggests that nanofibers in the spider silk fibers determine their unique mechanical properties [8, 9].

Recently, an electron microscopic examination of the spinning solution in *Bombyx mori* glands and the model in vitro experiments with regenerated natural silk have demonstrated that the silk protein molecules (including spider silk proteins) at a high concentration form micelles with a size of 100–200 nm, which assemble in large globules [8, 9]. Formation of these structures prevents a premature crystallization, thereby allowing hydrophobic proteins, which reach 2.5–3 thousand amino acid residues, to remain in the aqueous phase to a concentration of 40–45%. Presumably, the possibility of such structures to form is the most important element in simulating the fiber formation by silk proteins.

The folding of each spider silk protein, eventually leading to fiber formation (macro level), is an intricate multistage process with each stage requiring specific conditions [6, 7]. The spinning solution in spider glands passes the stage of “maturation,” and further transition from a preoriented liquid crystal solution into a mature fiber occur practically simultaneously as a result of a spinning event.

In the majority of cases, the silkworm fibroin is selected as a research object [4, 10, 11]. The advantage of recombinant analogs of spider silk proteins is in the possibility to change their mechanochemical and biological properties by selecting the corresponding amino acid sequences, which provides for creating the materials with prespecified properties. Numerous

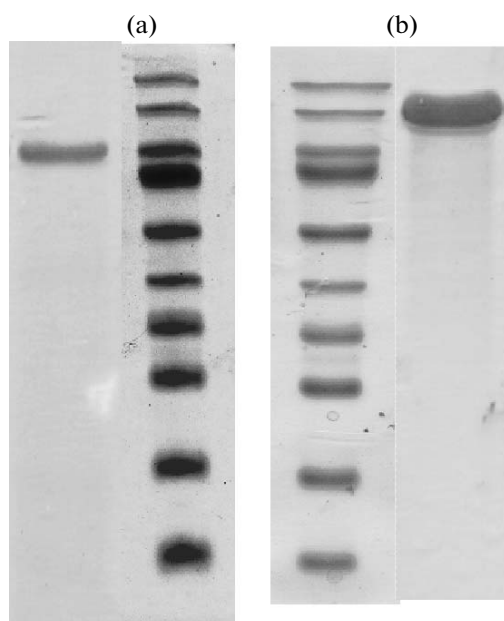


**Fig. 1.** Electrophoretic pattern of the purified proteins (a) 1F9 and (b) 2E12 (electrophoresis in 12% denaturing polyacrylamide gel; molecular weight standards (Fermentas, Lithuania) of 170, 130, 95, 72, 55, 43, 34, 26, 17, and 11 kDa).

papers describe the cloning of the spidroin genes in various expression systems, namely, cells of *Escherichia coli* [12], yeast *Pichia pastoris* [13], plants [14], and mammal cell culture [15].

We earlier synthesized and cloned in *P. pastoris* cells the genes with the nucleotide sequences maximally similar to the sequences of the genes encoding the natural proteins forming the dragline spider silk fibers, spidroins 1 and 2. The procedure for the isolation and purification of these proteins was also developed, and the structural transitions occurring in solutions of these proteins under the action of various factors were studied [16–18].

The goals of this work were to develop the methods for producing the fibers composed of recombinant analogs of spidroins 1 and 2 and study their properties as well as to compare their morphometric parameters and breaking strength. All stages of fiber production were controlled by scanning and transmission electron microscopies (SEM and TEM, respectively).

## EXPERIMENTAL

**Gene design.** The structures of artificial genes encoding protein analogs of spidroins 1 and 2 were modeled based on the known nucleotide sequences of natural genes: the gene *1f9* encoded the analog of spidroin 1 from the spider *Nephila clavipes* [19] and the gene *2e12* encoded the analog of spidroin 2 from the spider *N. madagascariensis* [20].

The monomers of recombinant genes were produced by chemical enzymatic synthesis and amplified within a vector. The final gene *1f9* contained nine

repeats of the corresponding monomer and encoded the protein with a molecular weight of 94 kDa [21, 22]. The gene *2e12* contained 12 repeats of the monomer and encoded the protein with a molecular weight of 113 kDa [18].

The resulting genes were inserted into the genome of the methane-oxidizing yeast *P. pastoris* under the control of the methanol-induced promoter AOX-1.

**Production and purification of the protein analogs of spidroins 1 and 2.** The producer yeast cells were grown in a fermenter in a periodic mode and destroyed in a ball grinder. Recombinant spidroins 1 and 2 (proteins 1F9 and 2E12) were isolated from the cell water-soluble fraction as earlier described [17], except that the HPLC was performed on a HiPrepSP column. The electrophoretic pattern (SDS PAGE) of purified proteins 1F9 and 2E12 is shown in Fig. 1. The bands with lower molecular weights correspond to the proteolysis products of the target proteins (demonstrated by immunoblotting; data not shown).

**Artificial spinning.** The artificial fibers were produced from the protein solutions according to our own technology [18] using the specially designed microspinneret with an outlet diameter of 20–50  $\mu\text{m}$  and a length of 3–4 cm. The weighed sample of freeze-dried protein was dissolved in a 10% solution of lithium chloride in 90% formic acid to a concentration of 20% and added in an amount of 1–2  $\mu\text{l}$  to the microspinneret. Under the pressure created by a peristaltic pump, the solution was extruded into a reservoir with a precipitation agent (96% ethanol) at a flow rate not exceeding 3  $\mu\text{l}/\text{min}$ . This resulted in the formation of the so-called as-spun fiber, freely hanging down to

the bottom of reservoir. After several centimeters of the fiber were formed, the pump was switched off, and the process was continued until the exhaustion of the solution.

**Fiber formation.** To improve the fiber quality, several stages were used, including extension of the fiber in 92% ethanol, extension in 75% ethanol, annealing at 180°C without fixation of the ends, plasticization in deionized water with elongation by 10% of the length, and air-drying in a fixed state. Three methods were used, which differed in the degree of fiber extension during the first two stages. The first method included extension by 25% of the initial length in 92% ethanol with subsequent elongation by 25% in 75% ethanol (in total, 1.72-fold). According to the second method, the fiber was extended by 100% in 92% ethanol with subsequent elongation by 25% in 75% ethanol (in total, 2.75-fold). In the third variant, the fiber was extended by 100% in each of the alcohols (in total, 4.4-fold).

**The breaking strength of fibers** was determined as follows. One end of the tested fiber was fixed, and a load with increasing weight was attached to the other end; the weight of the load causing the fiber break was recorded. The diameter of the broken fiber was measured by electron microscopy. The fiber breaking strength (hPa) was calculated as the ratio of the load weight (N) to the area of fiber cross-section ( $m^2$ ).

**Scanning electron microscopy (SEM)** was performed in a Camscan S2 (Cambridge Instruments) electron microscope in an SEI mode. The resolution of the microscope was 10 nm and working voltage was 20 kV. Before microscopic examination, the specimens were coated with a gold layer of approximately 20 nm in an argon atmosphere under an ion current of 6 mA and pressure of 0.1 mm Hg in an Ion Coater IB-3 (Eico, Japan) device. Each specimen was studied at two working magnifications, 1160 and 2430, to get overall and detailed images of the fiber. The images were recorded using an image digitization system with the MicroCapture software package (Sistemy dlya mikroskopii i analiza, Russia). The level of informationless noise was decreased by median filtration of the images.

**Transmission electron microscopy (TEM).** Fibers were fixed in 2% glutaraldehyde, postfixed in 2% osmium tetroxide in distilled water, contrasted with uranyl acetate in 70% alcohol, dehydrated in alcohols with increasing concentrations, transferred into acetone, and embedded into Epon mixture. Part of specimens was embedded into Epon mixture without fixation and staining. Ultrathin sections with a thickness of 6–7 nm were made using an Ultracat-R (Leica, Germany) ultratome, placed on copper grids with a Formvar support, and stained with lead citrate and 2% uranyl acetate. The sections were examined in a JEM-1011 (JROL, Japan) transmission electron microscope at a working voltage of 60 kV and magnifications of 50000 and 100000. The images were recorded using a Gatan ES500W digital camera with

the Digital Micrograph (Gatan, United Kingdom) software package.

The images were morphometrically processed with the help of the ImageScopeM program (Sistemy dlya mikroskopii i analiza, Russia).

## RESULTS

### Morphology of As-Spun Fibers

The so-called as-spun fiber is immediately formed in the case of an artificial spinning from concentrated spider solutions in 96% alcohol. This fiber is very fragile and displays no breaking strength. Such structures in the natural spider web are unknown. The as-spun fibers produced of the proteins 1F9 and 2E12 are morphologically indistinguishable.

SEM has demonstrated that the as-spun fiber displays a uniform thickness along its entire length (approximately 40  $\mu m$  in diameter) and a smooth surface with a few hollows (Fig. 2a) with a diameter not exceeding 2–3  $\mu m$ . It is evident in the cross-sections that the fiber has a tubular structure with a central cavity of up to 20  $\mu m$  in diameter surrounded by a spongy layer of 3–20  $\mu m$  (Fig. 2b–2d). The spongy layer has numerous pores with a diameter of 0.15–1  $\mu m$  (Fig. 2b, 2c). The pores on the angular sections remain round-shaped, suggesting that they are spherical. The fiber surface is osmiophilic, denser in its outer part as compared with the inner part and the inner pore surface. Part of the spongy layer protrudes into the cavity forming in some sites a “ridge” on the inner surface of the fiber (Fig. 2c).

Clusters of globular structures are located inside the cavity. The diameter of globules is 0.2–1  $\mu m$ . In cross-sections (Fig. 2d), the globules are protein structures with a somewhat condensed osmiophilic outer layer. The globular structures with a size of 50–250 nm were also observed on the surface of the as-spun fibers when producing the films of the protein 1F9 by casting in ethanol and when treating the hydrogel produced by this protein with methanol (data not shown). Such globular structures were earlier observed in the silk-worm spinning solution and in the ampullate glands of orb-web spiders [10, 23]. Note that 15-s treatment of the as-spun fiber with acetone leads to dissolution of the spongy layer, and only fibrillar structures with a thickness of approximately 20 nm remain.

### Formation of As-Spun Fibers

Extension of the as-spun fibers made of each of the proteins drastically changes their morphology (Fig. 3). The fiber diameter decreases, and thin fibers (which we named microfibrils) appear in them; the microfibrils are located in parallel to the main fiber axis (Fig. 3c, 3d; arrows). The microfibril diameter (200–900 nm) is approximately tenfold larger than that of the nanofibrils in the natural spider web (25–50 nm)

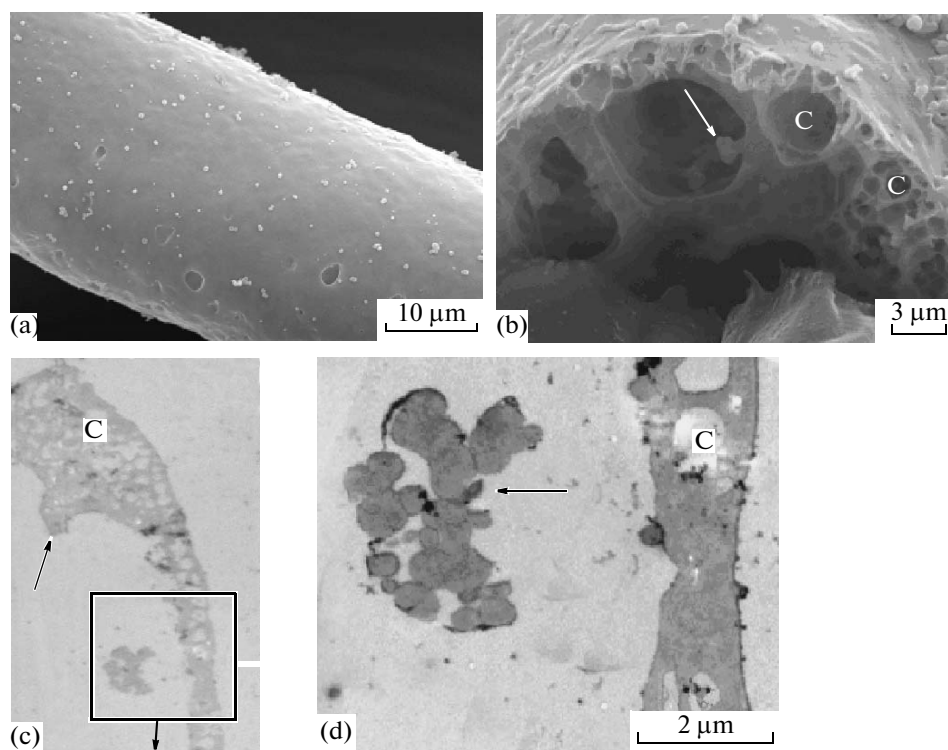


**Fig. 2.** Structure of the as-spun fiber (protein 1F9): (a) SEM image of outer fiber wall; (b) cross-fracture of the fiber (SEM), arrow indicates the globular structures within the fiber; (c) cross-section of the same fiber embedded into Epon (TEM), arrow indicates a protrusion of the inner wall; and (d) magnified image of part of 2c, arrow indicates a cluster of globular structures in the fiber internal cavity; C is the cavity in the fiber wall.

[8]. Such difference in the fiber morphology is explainable by an imperfection of the method used for artificial spinning. For comparison, note that the nanofibers produced by spinning of regenerated *B. mori* silk protein in a commercial device have a diameter of approximately 35 nm (observation of the authors).

When forming the fibers, the thickness of microfibrils changes insignificantly, whereas their length increases; the increase is most pronounced after the stage of plasticization in water (Fig. 4d).

**Morphology of formed fibers.** SEM of the extended fibers (Fig. 4a, 4b) demonstrates that the microfibrils are not uniform in their thickness but are rather moniform. With extension from 2.75- to 4.4-fold, a decrease in the mean thickness of microfibrils is observed along with a decrease in the mean fiber thickness (Fig. 5a, 5b).

The mean lengths of microfibrils made of the two studied proteins differ and depend on the method used for fiber production (degree of extension): it drastically increases in the case of a larger extension (method 3; Fig. 5c).

In the cross-section of the formed fiber embedded in Epon (Fig. 4c), the microfibrils are located over the

entire fiber area and are represented by protein structures with an osmiophilic outer layer.

A TEM examination of the fibers embedded into epoxy resin demonstrated the presence of clusters of osmiophilic inclusions in microfibrils; the inclusions had a diameter of 10–15 nm, were submerged into unstructured protein matrix, and located at a distance of approximately 20 nm from one another (Fig. 4c, arrows). Such structures were found in the cross-sections of the fibers made of both spidroins. In the longitudinal sections, elongated structures with a thickness of 20 nm and length to 250 nm were observed (Fig. 4d).

We have not found any statistically significant differences in the morphological parameters of the fibers caused by loading; however, the breaking strength of these fibers significantly differed: the fibers of the protein 2E12 were at least twofold more resistant to rupture (Fig. 5). The breaking strength increased with the total degree of extension (Fig. 6).

## DISCUSSION

The formation of artificial fibers of the recombinant analogs of spider silk proteins—a component of

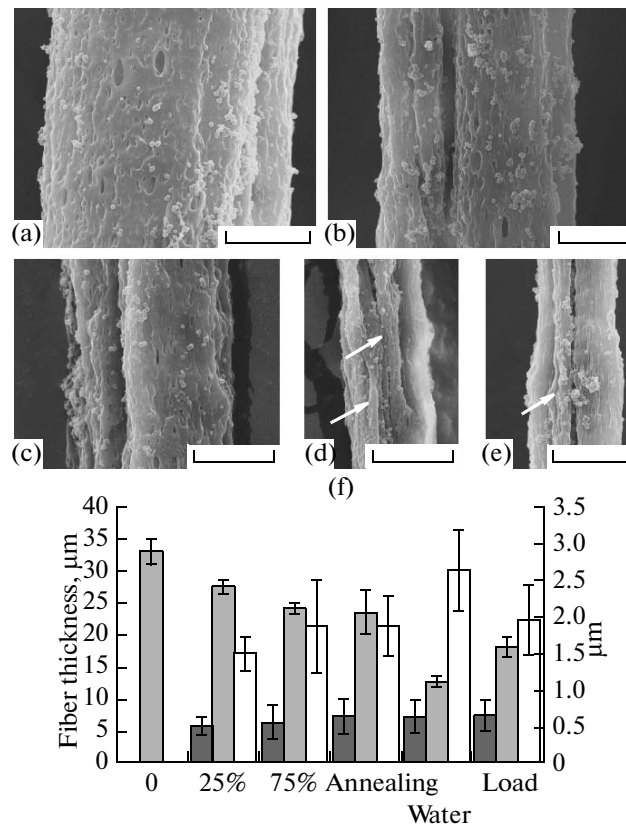


**Fig. 3.** Changes in the morphological parameters of the artificial spider silk fiber during its formation. (a)–(e) SAM images: (a) extension in 92% ethanol by 25%; (b) extension in 75% ethanol by 25%; (c) annealing; (d) plasticization in water, fiber 1; and (e) after loading (1 g), fiber 2. Arrows indicate microfibrils within the fiber, scale, 10  $\mu\text{m}$ . (f) Dependence of the fiber structure on the used extension method; light gray columns, fiber thickness; dark gray and white columns, thickness and length of microfibrils, respectively.

the developed model system for designing biomaterials with unique properties [18]—was studied.

We tried to reproduce the events taking place during natural spinning of the spider dragline silk fibers and partition them into several stages. Under natural conditions, several coordinated processes occur in the gland, namely, dehydration and removal of sodium and chlorine ions, introduction of potassium ions and protons, decrease in pH to 6.3, alignment of the molecules, structural transformations of  $\alpha$ -helices and poly-L-proline II-type structures into  $\beta$ -structure, and formation of  $\beta$ -sheet layers [24].

In our model, the as-spun fiber is an analog of the mature spinning solution at the last maturation stage of the spinning, when the phases enriched with polymer and enriched with solvent have already separated but the conformational transition of poly(A) blocks from an  $\alpha$ -helices to  $\beta$ -sheets have not yet occurred.

Elimination of the bound water in this model system (by analogy to the dehydration by reverse osmosis in the spinneret gland) is achieved by treating the fibers with alcohol solutions of decreasing concentrations (92 and 75%); presumably, successive extension

in such alcohol solutions brings the intercrystalline regions of spidroin molecules into an extended state oriented along the fiber axis (by analogy to the hydrodynamic shift in the spinneret gland).

The subsequent annealing at 180°C fixes this state. If the fibers are then placed into water, the fibers will partially shorten (supercontraction). This is explainable by the breaking of hydrogen bonds in water, which leads to the transition of the intercrystalline part of the molecules to a statistical coil. To avoid this, the fibers were treated with water (plasticization) after alcohol with fixed ends and additional extension by 10%. The additional fiber extension in water and drying in a fixed state leads to the appearance of microfibrils (Fig. 4a, 4b) and considerable improvement of their properties. Presumably, this is explainable by the fact that the extension in water causes an additional alignment of the molecules with one another and the formation of additional  $\beta$ -structures in the intercrystalline regions. This state is fixed during drying by the formation of new hydrogen bonds.

An ever increasing volume of data demonstrates that the nanofibers in the spider silk fibers provide for

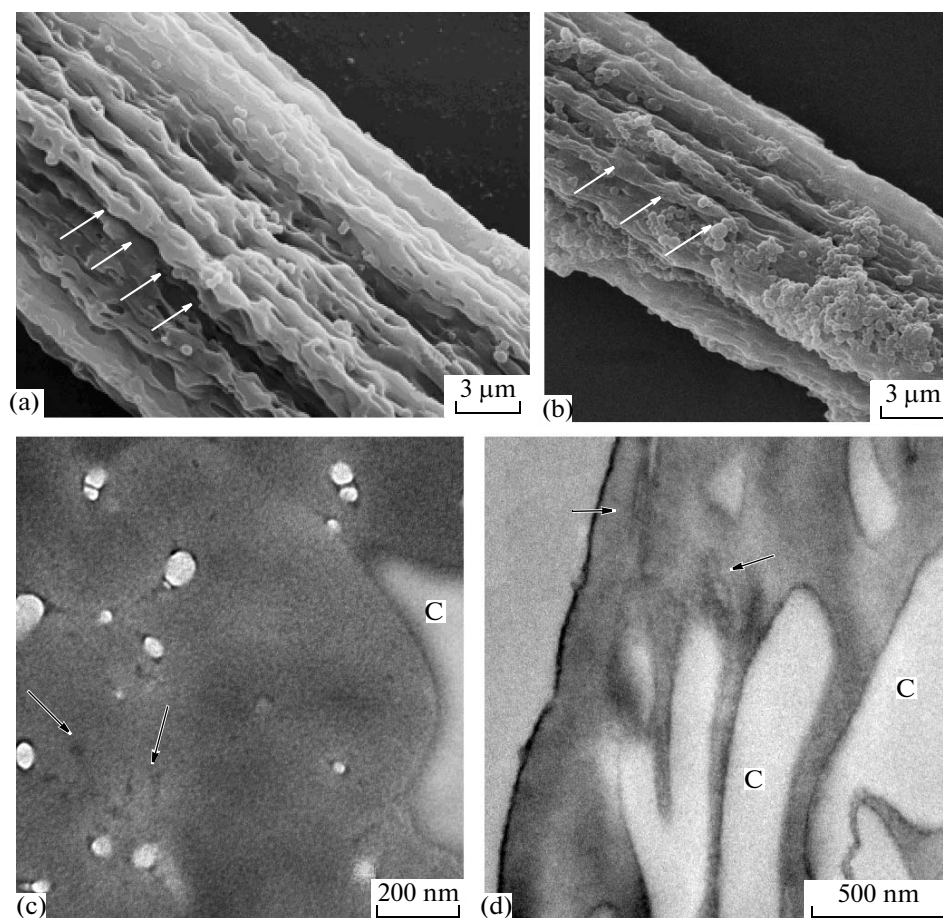


**Fig. 4.** Structure of the artificial fibers formed of spidroin analogs (method 1). SEM images of the fibers made of the proteins (a) 1F9 and (b) 2E12. Arrows indicate the globules within microfibrils. TEM images of (c) a cross-section and (d) a longitudinal section of the fiber (Fig. 3b) embedded into Epon. Arrows indicate osmiophilic inclusions; C is the cavity inside the fiber.

the unique spider web properties [4]. We observed osmiophilic inclusions with a diameter of 20 nm in the cross-sections of the formed fibers (Fig. 4c, 4d). There are no sufficient data to state that they are represented by clusters of nanofibers; however, note that the concentrated solutions of recombinant spidroins used for spinning contained large amount of nanofibers. Moreover, the fiber structures of the same diameter (20 nm) were observed after the as-spun fiber was dissolved with acetone. In the future, we plan to clarify how the presence of nanofibers in spinning solution influences the properties of the produced artificial fibers.

We have demonstrated that the breaking strength of the artificial fibers made of the proteins 1F9 (0.04–0.1 hPa) and 2E12 (0.05–0.17 hPa) differ and considerably increase with the degree in fiber extension (Fig. 5). These values are comparable to the data for recombinant spidroins [25]. On the other hand, the fibers of regenerated silkworm silk are twofold more resistant to rupture and of those of natural are tenfold more resistant than the fibers of the recombinant

spidroins [26, 27]. The diameter of the microfibrils composing the fiber decreases in the order recombinant spidroin–regenerated silk–natural fiber. It is natural to assume that a small microfibril diameter is among the important characteristic features correlating with a high breaking strength of the spider silk fiber. Consequently, we plan to select the conditions for artificial fiber spinning that would provide for a considerable decrease in the diameter of microfibrils. Analysis of the fiber breaking strength will allow this assumption to be tested.

Thus, our results demonstrate a feasibility of developing the biomaterials with unique properties using recombinant analogs of the spider silk proteins by imitating the natural spider web fiber spinning.

#### ACKNOWLEDGMENTS

We are grateful to T.E. Kramina and E.S. Trifonova for their assistance in statistical data processing. The electron microscopic examination was performed at

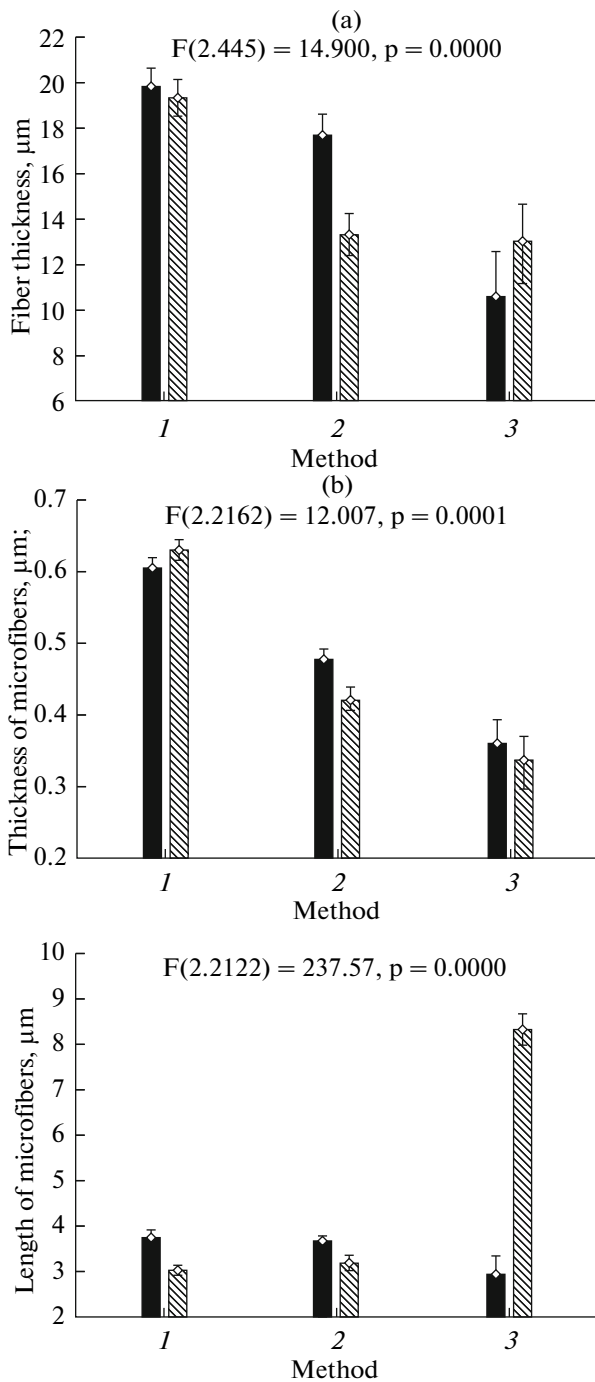


**Fig. 5.** The effect of the spinning method used (1–3) on the morphological parameters of the fibers made of the proteins 1F9 (dark columns) and 2E12 (stripped columns): (a) fiber thickness, (b) thickness of microfibers, and (c) length of microfibers.

the Laboratory of Electron Microscopy with the Biological Department of Moscow State University (head, G.N. Davidovich).

The work was supported by the Russian Foundation for Basic Research (project no. ofi-07-04-12172)

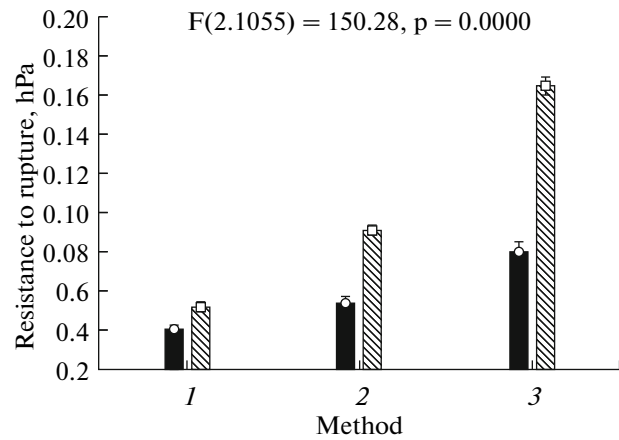


**Fig. 6.** The effect of the formation method (1–3) on the resistance to rupture of the synthetic fibers made of the proteins 1F9 (dark columns) and 2E12 (stripped columns).

and the Russian Federal Agency for Science and Innovations (FTsNTP GK no. 02.513.11.3384).

## REFERENCES

- Cunniff P.M., Fossey S.A., Auerbach M.A., Song J.W., Kaplan D.L., Adams W.W., Eby R.K., Mahoney D., Vezie D.L. 1994. *Nephila clavipes*. *Polym. Adv. Technol.* **5**, 401–410.
- Gosline J.M., Guerette P.A., Ortlepp C.S., Savage K.N. 1999. Mechanical properties of spider dragline silk: Humidity, hysteresis, and relaxation. *J. Exp. Biol.* **202**, 3295–3303.
- Kim U.J., Park J., Li C., Jin H.J., Valluzzi R., Kaplan D.L. 2004. Structure and properties of silk hydrogels. *Biomacromolecules*. **5**, 786–792.
- Kim K.-H., Jeong L., Park H.-N., Shin S.-Y., Park W.-H., Lee S.-C., Kim T.-I., Park Y.-J., Seol Y.-J., Lee Y.-M., Ku Y., Rhyu I.-C., Han S.B., Chung C.P. 2005. Biological efficacy of silk fibroin nanofiber membranes for guided bone regeneration. *J. Biotechnol.* **120**, 327–339.
- Haider M., Megeed Z., Ghandehari H. 2004. Genetically engineered polymers: Status and prospects for controlled release. *J. Controlled Release*. **95**, 1–26.
- Putthanarat S., Stribeck N., Fossey S.A., Eby R.K., Adams W.W. 2000. Reological characterization of *Nephila* spidroin solution. *Polymer*. **41**, 7735–7747.
- Du N., Liu X.Y., Narayanan J., Li L., Lim M.L., Li D. 2006. Design of superior spider silk: From nanostructure to mechanical properties. *J. Biophys.* **91**, 4528–4535.
- Vollrath F., Knight D.P. 2001. Liquid crystalline spinning of spider silk. *Nature*. **410**, 541–548.
- Jin H.-J., Kaplan D.L. 2003. Mechanism of silk processing in insects and spiders. *Nature*. **424**, 1057–1061.
- Chen X., Knight D.P., Vollrath F. 2002. Reological characterization of *Nephila* spidroin solution. *Biomacromolecules*. **3**, 644–648.

11. Furuzono T., Kishida A., Tanaka J. 2004. Nano-scaled hydroxyapatite/polymer composite. *J. Mater. Sci.* **15**, 19–23.
12. Fahnestock S.R., Irwin S.L. 1997. Synthetic spider dragline silk proteins and their production in *Escherichia coli*. *Appl. Microbiol. Biotechnol.* **47**, 23–32.
13. Fahnestock S.R., Bedzyk L.A. 1997. Production of synthetic spider dragline silk protein in *Pichia pastoris*. *Appl. Microbiol. Biotechnol.* **47**, 33–39.
14. Scheller J., Guühns K.H., Grosse F., Conrad U. 2001. Production of spider silk proteins in tobacco and potato. *Nature Biotechnol.* **19**, 573–577.
15. Lazaris A., Arcidiacono S., Huang Y., Zhou J.F., Duguay F., Chretien N., Welsh E.A., Soares J.W., Karatzas C.N. 2002. Spider silk fibers spun from soluble recombinant silk produced in mammalian cells. *Science*. **295**, 472–476.
16. Ragulina L.E., Makeev V.Yu., Esipova N.G., Tumanyan V.G., Nikitin A.M., Bogush V.G., Debabov V.G. 2004. Periodicities in the sequences of spidroins 1 and 2 from different spider species. *Biofizika*. **49**, 1053–1060.
17. Bogush V.G., Sazykin A.Yu., Davydova L.I., Martirosyan V.V., Sidoruk K.V., Glazunov A.V., Akshiina R.P., Shmatchenko N.A., Debabov V.G. 2006. Production, purification, and spinning of a recombinant analog of spidroin 1. *Biotekhnologiya*. **4**, 3–12.
18. Bogush V., Sokolova O., Davydova L., Klinov D., Sidoruk K., Esipova N., Neretina T., Orchansky I., Makeev V., Tumanyan V., Shaitan K., Debabov V., Kirpichnikov M. 2008. A novel model system for design of biomaterials based on recombinant analogs of spider silk proteins. *J. Neuroimmune Pharmacol.* **4**, 17–27.
19. Xu M., Lewis R. 1990. Structure of a protein superfiber: Spider dragline silk. *Proc. Natl. Acad. Sci. USA*. **87**, 7120–7124.
20. Motriuk-Smith D., Smith A., Hayashi C.Y., Lewis R.V. 2005. Analysis of the conserved N-terminal domains in major ampullate spider silk proteins. *Biomacromolecules*. **6**, 3152–3159.
21. Bogush V.G., Sidoruk K.V., Molchan O.K., Pti-tsyn L.R., Altman I.B., Kozlov D.G., Efremov B.D., Benevolenskii S.V., Agapov I.I., Mashko S.V., Debabov V.G. 2001. Molecular cloning and expression in yeast of synthetic genes encoding protein analogues of the dragline silk protein spidroin 1. *Biotekhnologiya*. **2**, 11–22.
22. Piruzyan E.S., Kobets N.S., Mett V.L., Serebriiskaya T.S., Neumyvakin L.V., Alizade Kh., Lenets A.A., Simonova M.L., Shevelukha V.S., Goldenkova I.V. 2000. Transgenic plants expressing foreign genes as a model for studying plant stress responses and a source for resistant plant forms. *Fiziol. Rast.* **47**, 370–381.
23. Slotta U., Hess S., Spiel K., Stromer T., Serpell L., Scheibel T. 2007. Spider silk and amyloid fibrils: A structural comparison. *Macromol. Biosci.* **7**, 183–188
24. Knight D.P., Völlrath F. 2001. Comparison of the spinning of selachian egg case ply sheets and orb web spider dragline filaments. *Biomacromolecules*. **2**, 323–334.
25. Fahnestock S.R. 1994. Novel, recombinantly produce spider silk analogs. *Int. Application #PCT/US94/06689*, *Int. Publication #WO 94/29450*.
26. Elices M., Perez-Rigueiro J., Plaza G.R., Guinea G.V. 2005. Finding inspiration in *Argiope trifasciata* spider silk fibers. *J. Minerals Metals Materials Soc.* **57**, 60–66.
27. Seidel A., Liivak O., Calve S., Adaska J., Ji G., Yang Z., Grubb D., Zax D.B., Jelinski L.W. 2000. Regenerated spider silk: Processing, properties, and structure. *Macromolecules*. **33**, 775–780.